

## Article

# Late Holocene Morphodynamic Feedback in Can Gio Mangrove Tide-Dominated River Mouth Systems, Vietnam

Thuyen Xuan Le <sup>1,2,†</sup>, Klaus Schwarzer <sup>3,\*</sup> , Thanh Cong Nguyen <sup>2,4</sup>, Luan Thi Bui <sup>2,5</sup> and Daniel Unverricht <sup>6</sup> <sup>1</sup> Department of Ecology and Evolutionary Biology, University of Science, Ho Chi Minh City 72711, Vietnam<sup>2</sup> Vietnam National University, Ho Chi Minh City 72711, Vietnam<sup>3</sup> Coastal Geology and Sedimentology, Institute of Geosciences, Kiel University, 24118 Kiel, Germany<sup>4</sup> Department of Oceanology, Meteorology and Hydrology, University of Science, Ho Chi Minh City 72711, Vietnam<sup>5</sup> Department of Marine and Petroleum Geology, University of Science, Ho Chi Minh City 72711, Vietnam<sup>6</sup> Marine Geophysics and Hydroacoustics, Institute of Geosciences, Center for Ocean and Society, Kiel University, 24118 Kiel, Germany

\* Correspondence: klaus.schwarzer@ifg.uni-kiel.de

† This article is dedicated to our always inspiring colleague Thuyen Xuan Le, who initiated this contribution but passed away in 2022 during the late stage of the preparation of this manuscript.

**Abstract:** Can Gio (CG), a mangrove forest with a dense network of tidal creeks, gradually grew and spread seaward on a coastal platform, which was built since about 8 ka before present (BP). Along with this development, a sand ridge began to form and moved back with the shoreline withdrawal landward in the Late Holocene. This mangrove environment is likely abandoned from the mainland but was, however, the place for settlement of ancient Vietnamese a few centuries BC. The CG mangrove forest was severely destroyed during the American War and was restored since 1980. However, the historical change of the landscape along the Saigon-Dong Nai River (SG-DNR) since the Late Holocene is not completely unraveled. By analyzing sediment cores with a multiproxy approach, we investigated the recent geological development with regard to the variation of the intensity of the East Asian palaeomonsoon and regarding the accommodation space, as both regulate the development of this coastal environment. A recently significant shift in the coastline, mainly due to a change of hydroclimatic factors, was observed. A continuous coastline retreat occurred over the last millennium, changing the depositional environment and reshaping the CG mangrove landscape. Along the present coast and tidal channels, partially strong erosion and bank failures occur, alternating with accretion at other coastal sections. This development tends to increase progressively.

**Keywords:** Can Gio mangroves; mangrove coast evolution; back barrier development; sand ridge; coastal morphodynamics; pre-Oc Eo culture



**Citation:** Le, T.X.; Schwarzer, K.; Nguyen, T.C.; Bui, L.T.; Unverricht, D. Late Holocene Morphodynamic Feedback in Can Gio Mangrove Tide-Dominated River Mouth Systems, Vietnam. *Coasts* **2022**, *2*, 221–243. <https://doi.org/10.3390/coasts2030011>

Academic Editor: Brooke Maslo

Received: 5 April 2022

Accepted: 26 July 2022

Published: 17 August 2022

**Publisher's Note:** MDPI stays neutral with regard to jurisdictional claims in published maps and institutional affiliations.



**Copyright:** © 2022 by the authors. Licensee MDPI, Basel, Switzerland. This article is an open access article distributed under the terms and conditions of the Creative Commons Attribution (CC BY) license (<https://creativecommons.org/licenses/by/4.0/>).

## 1. Introduction

A coastal area is the interface between the air, the land and the sea, where landforms are continuously changing due to the interaction between the different driving forces. This occurs especially in river-mouth environments where a large amount of material is discharged and exchanged and where also a “sink” for matter, deriving from the catchment area, exists. The characteristics of typical sedimentary processes occurring in these river-mouth systems are already generalized [1–3]. Mangroves, which develop in the intertidal zone of tropical and subtropical coastlines, represent a specific ecosystem in these environments [4–6].

The development of most Asian deltas started with the deceleration of the postglacial sea-level rise at about 8000 ka. Progradation increased rapidly after the Holocene sea level highstand of +1.5 m was reached between 6.7 and 5.0 ka before present (BP) [7,8], with a peak value at 6.0 ka BP and falling slowly to the present level. The amount of

sediment discharge, the geomorphological configuration of the basin as well as tide and wave processes control the development of a delta. Therefore, a switch from a tide to a more wave-dominated delta was observed for the Mekong River Delta (MRD) when the coastline was migrating towards S–SE, leaving the shelter from the rocky mainland, of which Vung Tau Peninsula is the southwestern most extension (see Figure 1), against wave attacks from the northeast.

In terms of hydrology and geomorphology, the SG-DNR is an upper mesotidal environment with diurnal tides reaching up to 4 m tidal range and displaying pronounced estuarine conditions (Figure 2). This area is encircled by the largest protected mangrove forest in southern Vietnam. The nature of this ecosystem has generally been described, based on recent data of the forest structure, ecosystem services and also the physical characteristics of the intertidal environment including climate, geomorphology, topography and hydrology [9–15]. Moreover, archaeological remnants have been used to describe the development of this landscape [16].

While heavily damaged during the American War lasting from 1954 to 1975, this area was subsequently reforested [9]. By evaluating the state of the CG mangrove's biosphere reserve (Figure 1) after 40 years, the recovery of the biodiversity is considered to be excellent. CG mangrove environment is now back, and it is a forest inside the most diverse mangrove regions of the world [17,18]. In this area, river distributaries are the main gateways from the ocean to Ho Chi Minh City (HCMC), the largest industrial city in South Vietnam, with more than  $200 \times 10^6$  tons of cargo transported each year on these waterways.

The south of this river-mouth system borders directly with the well-studied MRD (see review by Anthony et al., 2015 [19]), which is the third largest delta plain on a global scale [20]. With respect to a water discharge of  $450\text{--}550 \text{ km}^3/\text{yr}$ , it ranks the seventh [21], and with respect to a sediment discharge of  $150\text{--}160 \text{ Mt/yr}$ , it is the eleventh largest delta [21,22]. In contrast to the MRD, in CG region only limited but different studies have been carried out concerning biotic-abiotic conditions [23,24], land subsidence [25] or historical pollution related to the industrialization in the catchment area [13,14,26]. Some studies about the Holocene coastal evolution have been combined with studies of the MRD [27], where CG region is often considered just as an appendage or “marginal basin” of this huge delta [28,29]. However, even if both systems have completely different distributaries and geomorphological conditions in the vicinity, an independent geomorphological and sedimentological evolution of the SG-DNR has not been considered up until now.

Although the CG region is located adjacent to the large MRD in the southwest and is limited by the rocky coast of Vung Tau Peninsula (Figure 1) and an old terrace on the eastern side, the specific disparity in the development process between these large depositional landforms has not been clarified yet. There are different opinions about the origin of the sediment, which builds up CG region. While Szczucinski et al. (2013) [30] and Xue et al. (2014) [31] assumed that sediment is transported as suspension loads during the SW monsoon from the Mekong River mouth towards CG region, Collins et al. took some sediment inputs from the Saigon-Dong Nai River system into account. However, no evidence is shown for this assumption. Investigations of the present sediment distribution in the river channels [32] exhibit a gradient from fine- to coarse-grained sediment upstream, indicating the partly rocky hinterland as a potential sediment source.

Regarding landforms along the broad soft rock coast and mangrove forest of the SG-DNR, there are different types of geomorphological features such as active cliffs and mobile sandbanks, all characterizing a dynamic coast. The change of those landforms as well as strong erosion, bank failures and high deposition, extending largely along the coast and the tidal channels, occurred continuously for at least several decades [15,33,34]. Currently, the question about the occurrence of these dynamic processes, even destructive processes, and their long-term impacts in the history of CG area is still unanswered.



**Figure 1.** The study sites of different projects [14,26–28,35] in the Saigon-Dong Nai river-mouth area, Can Gio mangrove reserve. Details of own investigations are shown in the rectangle (see Figure 3). Sources of the hybrid image: Earthstar Geographics, Esri, Garmin, FAO, NOAA, USGS, available online, accessed on 4 July 2022.

This study investigates the coastal evolution on different time scales [36] from the mid-Holocene to the present epoch and the depositional processes occurring near the northeastern edge of the MRD, which is currently the most dynamic part of the CG area. Additionally, this study aims to clarify the mechanism that regulated the historical and present development of CG region. Whether the development of the MRD and SG-DNR happened simultaneously and if/when and in which way both systems merged is currently still in question. A conceptual model of the landscape evolution during the last 2500 years will be developed. Up until now, the sediment source from which the subsurface of CG region was built up is still unknown.

Our interpretation will focus on (1) the origin of sediments building up CG region, (2) the evolution of the sedimentary environment in space and time, (3) the coastal dynamics related to climatic fluctuation on a regional scale and (4) the geomorphological evolution of the CG region since the Late Holocene. The interpretation will be based on a combination of the available data. Our study mainly focusses on the central mangrove patch (Figure 1),

which is most advanced towards the sea and most dynamic in terms of sediment mobility and geomorphology.

## 2. Materials and Methods

### 2.1. Regional Settings

CG region is a low-lying coastal area with a plain topography ranging from  $-0.3$  to  $2$  m above the mean sea level [9]. It is located on the northeastern margin of the MRD in the estuarine part of the SG-DNR system, which discharges into the East Sea (South China Sea) through an intricate system of river distributaries and tidal creeks (Figure 1). The area of CG has been broadly ruined by defoliants that were sprayed during the American War (1954–1975). However, mangrove restoration has been successful since 1978, and in the year 2000, the CG forest was recognized by UNESCO as the first Biosphere Reserve in Vietnam [9]. Currently, this mangrove forest covers about  $40.3$  km<sup>2</sup>.

After the Holocene sea-level highstand was reached (6.7–5.0 ka BP), it dropped almost linearly to present-day conditions modulated by small-scale climatically induced oscillations [8,37]. Since 5.5 ka BP, the MRD has been prograding southeast and southward for up to  $250$  km due to the sea-level drop and fluvial sediment supplies [38]. Based on grain size variations of sediment samples taken from boreholes [39–41] and the occurrence of beach ridge systems on the subaerial delta [42], it could be shown that, ca. 3.0–2.5 ka BP, the delta evolution experienced a phase shift from “tide-dominated” to “tide-and-wave-dominated” conditions, causing changes in the subaqueous delta morphology, sediment facies, subaerial delta topography and progradation rate [42,43].

The river system of SG-DNR has a total drainage area of about  $46,000$  km<sup>2</sup> [32], which is only ca. 5.5 % of the Mekong River Basin [27,32], and an annual water discharge of about  $21 \pm 8$  km<sup>3</sup> [29], which is about 5% of the Mekong River discharge [21]. This discharge changes seasonally due to the monsoon regime. The study area with its irregular semidiurnal tides is under the influence of the seasonally opposite East Asian Monsoon (EAM) and South Asian Monsoon (SAM), which are, due to their directions of propagation, called NE and SW monsoon.

In the East, about  $20$  km across Ganh Rai Bay, the rocky headland of Vung Tau Peninsula acts as a natural shield for the CG area against waves induced by the NE monsoon (Figure 1). Towards west-southwest directions, the flat topography of the MRD borders the CG area.

According to the classification scheme developed by Galloway [44], the CG area can be regarded as a tide-dominated delta with a strong estuarine character. It comprises a dense system of distributaries and tidal channels downstream, which extend along the lower reaches of the SG-DNR. The shoreline is fragmented by two shallow bays, Ganh Rai Bay in the east and Dong Tranh Bay in the west (Figure 1), where the MRD takes course beyond the western margin. Along the coast between Ganh Rai Bay and Dong Tranh Bay, a unique beach-ridge complex with a width of  $0.5$ – $1.5$  km and a length of about  $10.5$  km borders the CG area to the southeast. This barrier is formed by recurved beach ridges [28].

The water regime of the study area is strongly affected by a mixed, mainly semidiurnal tide with a maximum tidal range of  $4$  m during spring tide [12,45]. On the seasonal scale, these tides are interacting with the contrasting NE and SW monsoon-induced rainfall and wind speed and wind direction [12]. The mean daily and seasonal water level variations at Vung Tau station for the period from 1991 to 2009 are shown in Figure 2. Currently, there is a dominance of monthly wind speed and high-water levels during the NE monsoon, intensifying the energy input by offshore wind and waves approaching the coast during this season. Figure 2 shows that waves are much higher during the NE monsoon, resulting in a stronger energy input to the coast.

The key features in the regional structural geology are known from investigations carried out more than 30 years ago [46]. Details of the sedimentary facies and structure of the Holocene strata have been documented recently [27,28]. Regarding the results of several studies (see caption in Figure 1), the multiple dates of the radiocarbon age of

intertidal deposits are bracketed between ages of 400 and 2600 cal. BP, as recorded in many sites [27,28]. The sediment accumulation rate assessed using  $^{210}\text{Pb}$  analyses demonstrates that, additionally, enormous recent accretion inside the mangroves with a rate of 2.9 cm/yr for the last 34 years occurs [14,26]. This relatively high sedimentation rate supports a rapid expansion as observed in many places inside the CG region, such as in the Khu Can Cu Vam Sat (in the square in Figure 1) from 1957 to 2001 [47]. In contrast, the coastal sections exposed directly to the sea and in the lower river courses have been strongly affected by unabated marine abrasion in recent decades, which is observed mainly in Ganh Rai Bay [34] along the eastern side of CG [48] but as well along the coast of the Dong Tranh River [15]. Here, the coastline experiences continuous intense erosion, especially along the navigation channels [33]. Currently, intensive riverbank collapse occurs along the three large rivers, Thi Vai, Long Tau and Soai Rap, which are the main navigation channels crossing CG and leading to the major ports in South Vietnam.

Our study was carried out at the mouth of the Dong Tranh River and the adjacent mangrove forest (Figures 1 and 3). Some additional surveys were carried out in other areas of the CG (Figure 1).

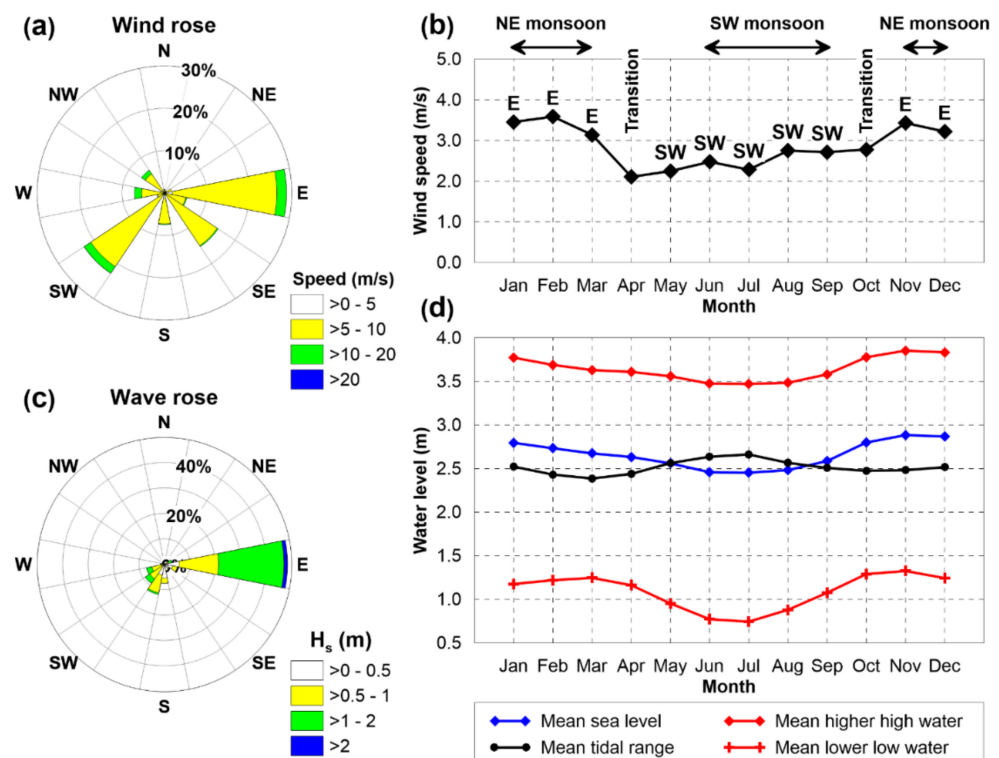


**Figure 2.** Monsoonal wind (a,b), wave (c) and water level fluctuations (d) in the study area. Wind data (1999–2008) and data of monthly mean water levels (1991–2009) are obtained from Vung Tau Metro-Hydrology station, operated by the Southern Regional Hydro-Meteorological Centre. Offshore wave data (2011–2020) are taken from Wavewatch III (location: 9.0 N, 107 E, [https://pae-paha.pacioos.hawaii.edu/erddap/griddap/ww3\\_global.html](https://pae-paha.pacioos.hawaii.edu/erddap/griddap/ww3_global.html), accessed on 1 January 2022). Waves are at the highest during the NE monsoon (c).

## 2.2. Archaeological Sites

Furthermore, many archaeological sites belonging to the coastal community of the pre-Occochean culture have been discovered in CG [49]. There are several prominent mounds, built up with basaltic soil, which are 1–3 m higher compared to the surroundings. Here, many ceramic objects and jar-burials, buried at the sites Cavo and Phet mounds (Figure 1), have been discovered, showing radiocarbon ages of  $2400 \pm 480$  and  $2100 \pm 50$  years BP, respectively [49]. In archaeological collections, the settlement of this culture in the MRD

region is well-known [50,51]. However, why these ancient people were settling here in a frequently flooded lowland rather than on the more advantageous high terrain of the sand ridge and the reason for its end still remain unknown.

### 2.3. Materials and Methods

To obtain detailed information about the geological, geomorphological and sedimentological evolution, we obtained nine sediment cores (for location see Figure 3) by gravity coring (PVC tube, 9 cm diameter) in 2005. The platform for coring in the river was a fishing boat. For all coring processes, no technical device was used but only a weight, which was moved up and down by manpower. With this technique, a maximum penetration of 3.90 m was achieved.

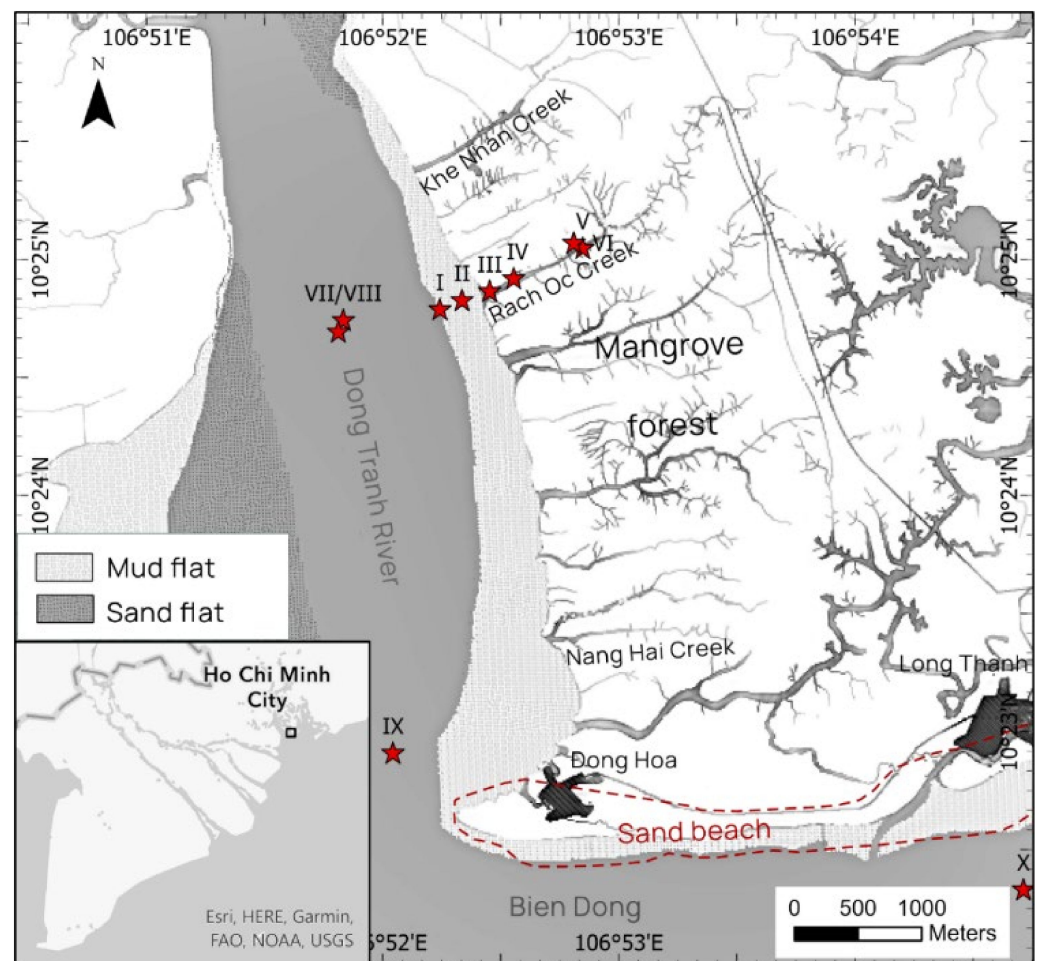


**Figure 3.** Main sampling sites in the Dong Tranh estuary (for section see Figure 1). Red stars are own coring sites.

Cores from location I to VI were taken successively along a profile in the intertidal environment from the low water mark on the tidal flat to the mangrove forest. Core VI was taken in the mangrove environment right at the bottom of the Rach Oc tidal creek, while core V was located in the nearby *Rhizophora* forest (Figure 4). From the soil surface (core V), which is flooded only during spring tide, to the bottom of core VI, approximately 7 m of continuous mangrove deposits was penetrated. Core IX was taken in the river mouth from the bottom of the Dong Tranh river at a depth of about –10 m. In addition, 40 grab samples of bottom sediments from Long Tau and Soai Rap channels, taken for the implementation of a dredging project in 2013 and 2016 (maintenance and dredging of the Soai Rap river channel), are included in this study.

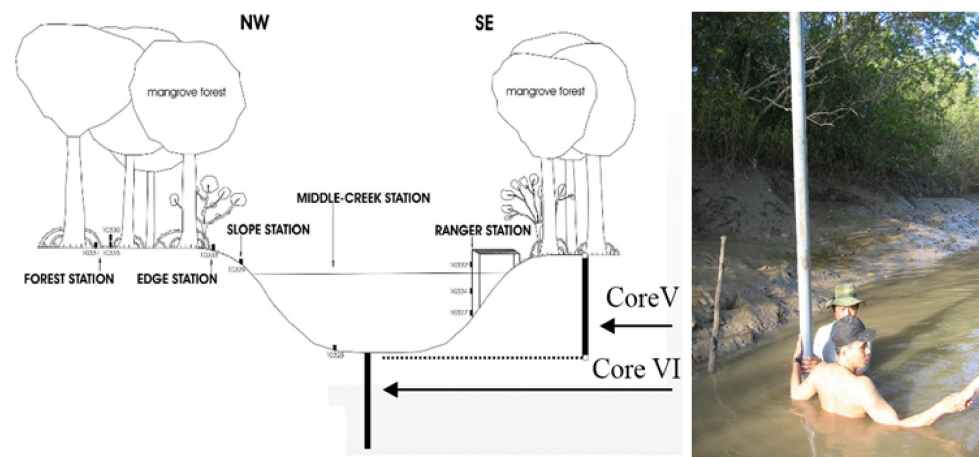


**Figure 4.** Sketch of the position of sediment cores V (in the forest) and VI (in the creek). The different locations termed “station” are positions to measure suspension load in the water column for the Project SEDYMAN. The picture to the right shows the coring procedure in the Rach Oc tidal creek. Length of core V: 3.90 m; length of core VI: 3.53 m.

Shallow seismic measurements along profiles in shallow water were carried out close to CG. One profile was conducted in south-north direction in the mouth of the Dong Tranh River channel (see Figure 5 in results). Seismic data were acquired in 2007 onboard a fishing boat by using a Boomer system comprising a 150–450 J power supply (CEA Pulsar 2002), a sound source mounted in a catamaran (manufactured by EG&G) and an 8-element single channel streamer. The devices were towed behind the ship at a distance of about 30–40 m to the GPS antenna. Boomer data were recorded using the software NWC 1.4.1 (Nautic Seismic Recording System) by Nautik Nord GmbH. Two-way travel times were converted to depths using a sound velocity of 1500 m/s for the water column and the upper layers of the seafloor. Data were processed by applying a Butterworth bandpass filter with 400 Hz as the lower and 6000 Hz as the upper cutoffs.

The sediment cores, taken in the frame of the research project SEDYMAN, were split vertically in the Vietnam National Center for Natural Science and Technology, Subinstitute of Geography. Both halves were photographed and described regarding its structure, texture, lithological composition and the occurrence of microbenthic species. For further analyses, one half of the sediment core was shipped to the Institute of Geosciences, Coastal Geology and Sedimentology of Kiel University (IfG) for taking X-rays, grain size analyses and for age control by radiocarbon dating. Subsamples were collected from the other half and were sent to the laboratories of Geology of the University of Sciences in HCMC for the analysis of the microfauna. In addition, the samples of cores V and IX and one more sample from the Pleistocene basement at 18 m core depth of core X (taken from the intertidal outer sand beach, Figure 3), provided by the embankment-coastal protection project, 2004, was used for the analysis of clay minerals.

Grain size characteristics of the sediments were determined by using a laser size analyser (LS13320, Beckman Coulter) at IfG with a measuring range of 0.04 to 2000  $\mu\text{m}$ . Therefore, grains larger than 2000  $\mu\text{m}$  were separated before the measurements. Additionally, prior to grain size analyses, the samples were treated with  $\text{H}_2\text{O}_2$  and HCl to remove organic matter and carbonate. To avoid any particle aggregation during the measurement,  $\text{Na}_4\text{P}_2\text{O}_7$  was added. The statistical parameters of the grain size distributions were calculated using the logarithmic method of moments available with the GRADISTAT software [52]. The sediment’s classification is based on the Folk classification scheme [53].

The provenance of sediments is demonstrated through the application of clay mineral analysis, conducted by X-ray diffraction at the Center for Research and Development of Safety and Environment Petroleum in HCMC. Clay minerals were determined according to the common technical instruction developed by Holtzapffel [54] using the clay fraction

(<2  $\mu\text{m}$ ). The identification of minerals was performed based on the appearance and intensity of the characteristic peaks of each mineral in the X-ray diffraction spectrum.

Foraminiferal species were selected using a 45  $\mu\text{m}$  sieve and determined under a microscope. The ecological characteristics of the given sediment layer were interpreted based on indicator groups of foraminifera and by applying a confinement index  $I_c$ , which is a quantitative index calculated on the basis of foraminiferal assemblages. The Index  $I_c$  is sensitive to slight changes in the environmental characteristics [55], and it is used as a sensitive tool to quantify the indication of changes in the paralic environments between more restricted ( $I_c$  increases) or less restricted ( $I_c$  decreases) conditions. Its metric is determined according to the calculation described in earlier results for the Mekong Delta and the CG region [23,56].

Age control by radiocarbon dating of shell and wood fragments of 9 samples was carried out by the AMS (Accelerator Mass Spectrometry) method in the Leibniz-Laboratory for Radiometric Dating and Stable Isotope Research of Kiel University (Germany). The conventional radiocarbon age was calculated according to Stuiver and Polach [57], with a correction for the effects of method-based isotope fractionation. The conventional ages were calibrated using OxCal V4.2 [58] and the calibration was set to IntCal13 [59]. The ages are presented in calendar years BP with a 95% confidence interval (Table 1).

Data about short term sedimentation were provided by the land subsidence monitoring by using the SET-MH technique [60], which was established at two locations: one in the mangrove forest (July 2010) and another in a forest gap (June 2011). Around each location, nine artificial marker-horizons and 3 steel rods for measuring the elevation change were used to estimate the amount of new sedimentation. Those stations are attributed to the USGS-VNU joint research project “Research and monitoring of coastal vulnerability and climate change”, which has been ongoing since 2010. Here, we only report the data of sedimentation, which were recorded at the mangrove forest location.

### 3. Results

#### 3.1. Sediment Characteristics, Provenance and Interpretation of Their Deposition

The unique sand ridge, which exists along the southernmost coast of the CG area (Figure 1), is about 2 m high and is composed mainly of fine to medium sand. The eastern part of the ridge is narrow and widens, similar to a feather in its western part, reflecting its direction of growth. Landward of this sand ridge, the sediments in cores V, VI and IX (Figure 3) are distinctly different. They mainly consist of finer particles, except the lower part of core IX, which consists of coarse-grained calcareous nodules (Figure 5). Similarly, fine-grained sediments, mostly clay and silt, are documented in previous studies that were carried out in CG region (Figure 1) [27,28]. The occurrence of fine-grained sediments indicates that the deposits below the mangroves were formed in a low-energy estuarine environment. The angular calcareous nodules at the base of core IX (Figure 5) are interpreted as a neo-formation, resulting from early diagenesis in an anoxic marine environment [61]. In addition, the bottom sediments in the three main river distributaries Soai Rap, Dong Tranh and Long Tau consist of silt, while sand only accounts for a low content in cores with a length of 1.5–2.0 m, which were taken in 2014 for the project “dredging the Soai Rap channel” (Figure 1).

Clay minerals are good indicators of sediment provenances [62]. The assemblage of clay minerals in the sediments of CG shows the presence of Kaolinite, Illite, Smectite and Chlorite, identified by characteristic peaks at 7 Å (Kaolinite), 10 Å (Illite), 14 Å (Chlorite) and 17 Å (Smectite), respectively (Figure 6). Based on the intensity of characteristic peaks, the amounts of Kaolinite, Illite and Smectite are present with more than 30%; the amount of Chlorite is less than 10%. The percentage of Smectite slightly decreased in the surface layer (0.07–0.10 m) as well as in the recent sediment of core IX.

Regarding the position of core IX in the seismic profile (Figure 5), its lower calcareous layer is interpreted as part of a horizontal bed overlying consolidated strata. Above this

bed, soft grey–brown and fine-grained sediments appear at the base of core V and in core VI, which are both, regarding the morphological level, above core IX.

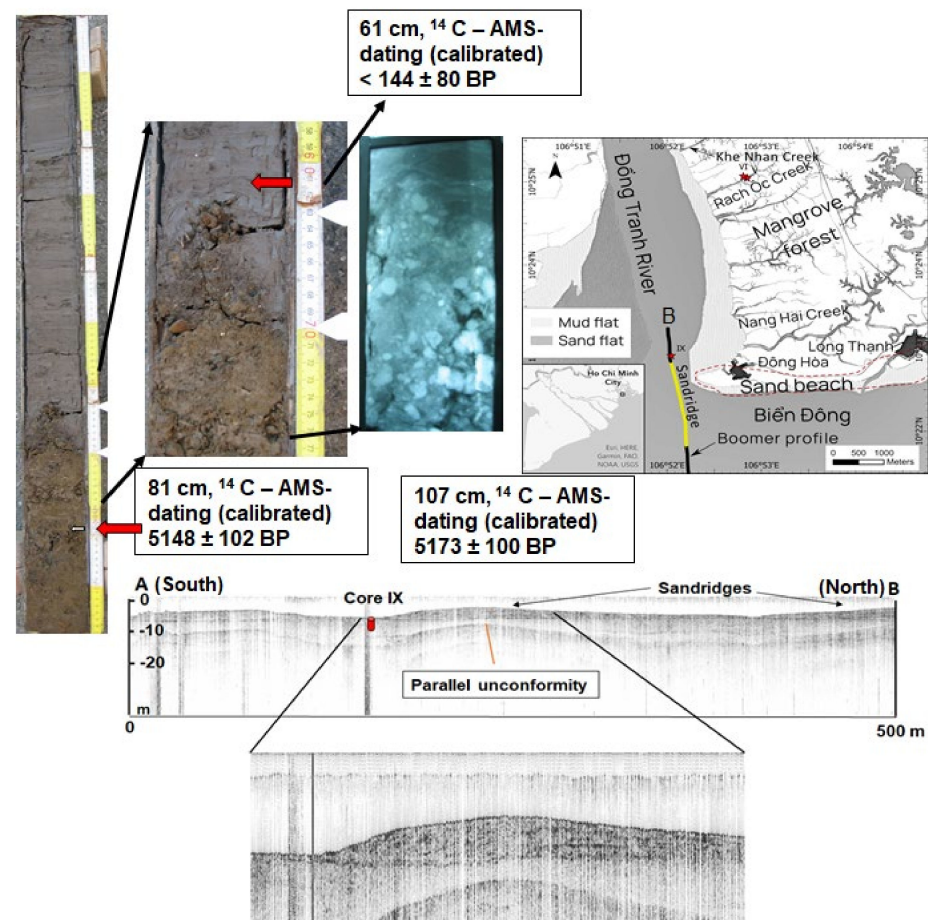


**Figure 5.** Unconformity at the base of core IX, which was taken in the mouth of the Dong Tranh River, and a south-north-directed seismic profile (A-B) recorded in this channel. The photo of the core reaches only down to 100 cm. The lithology and sedimentological composition down to 107 cm—not shown in the core-photo—where a shell fragment for AMS-dating was taken did not change.

Foraminiferal assemblages along the cores demonstrate a common trend in the depositional environment. There are three groups of foraminifera in all samples with their own characteristics among 44 species, which are discovered in total. Group A includes *Asterorotalia dentata*, *Asterorotalia pulchella* and *Brazalina striatula*, characterizing strong marine influence. Group B includes *Ammonia* spp., *Brazalina* cf. *variabilis* and *Quinqueloculina seminula*, representing moderate continental influence, while group C is typical for high continental influences based on the abundance of *Ammotium* cf. *salsum*, *Arenoparrella asiatica*, *Haplophragmoides wilberti* and *Trochammina* spp.

At the location of core IX, a relatively restricted environment already existed before 5.2 kyr BP (Figure 5, Table 1) as indicated by the presence of calcareous nodules as neoformation in an anoxic marine environment, but the foraminifera of B-group were relatively abundant. Subsequently, the marine influence prevailed and the amount of sedimentation was very low at this site. As the thickness of the young uppermost layer outside the sandridge amounts to only 60 cm, deposited during the last  $144 \pm 80$  years (Figure 5), there is a hiatus for about 5.0 ka at this position in the river mouth.

Asymmetric sandridges with the steeper slope directing south indicate a north-south sediment transport in the river mouth at the present seafloor. These bedforms are up to 4 m high and reach a length of about 240 m. Those structures are typical for ebb-dominated estuaries where sediment is transported towards the open sea.

Given that cores V and VI together comprise approximately 6 m of subtidal deposits, which were deposited from about  $0.474 \pm 48$  ka BP to  $0.185 \pm 80$  ka BP, the rate of sedimentation estimated for this site amounts to about 1.5–2 m/century, which is quite high for back-barrier conditions. Thereafter, with the deposition of intertidal deposits under mangrove colonization, the accretion decelerated to about 0.6 m/century based on the chronological data of radiocarbon dating obtained from the sediment cores V and VI (Table 1).

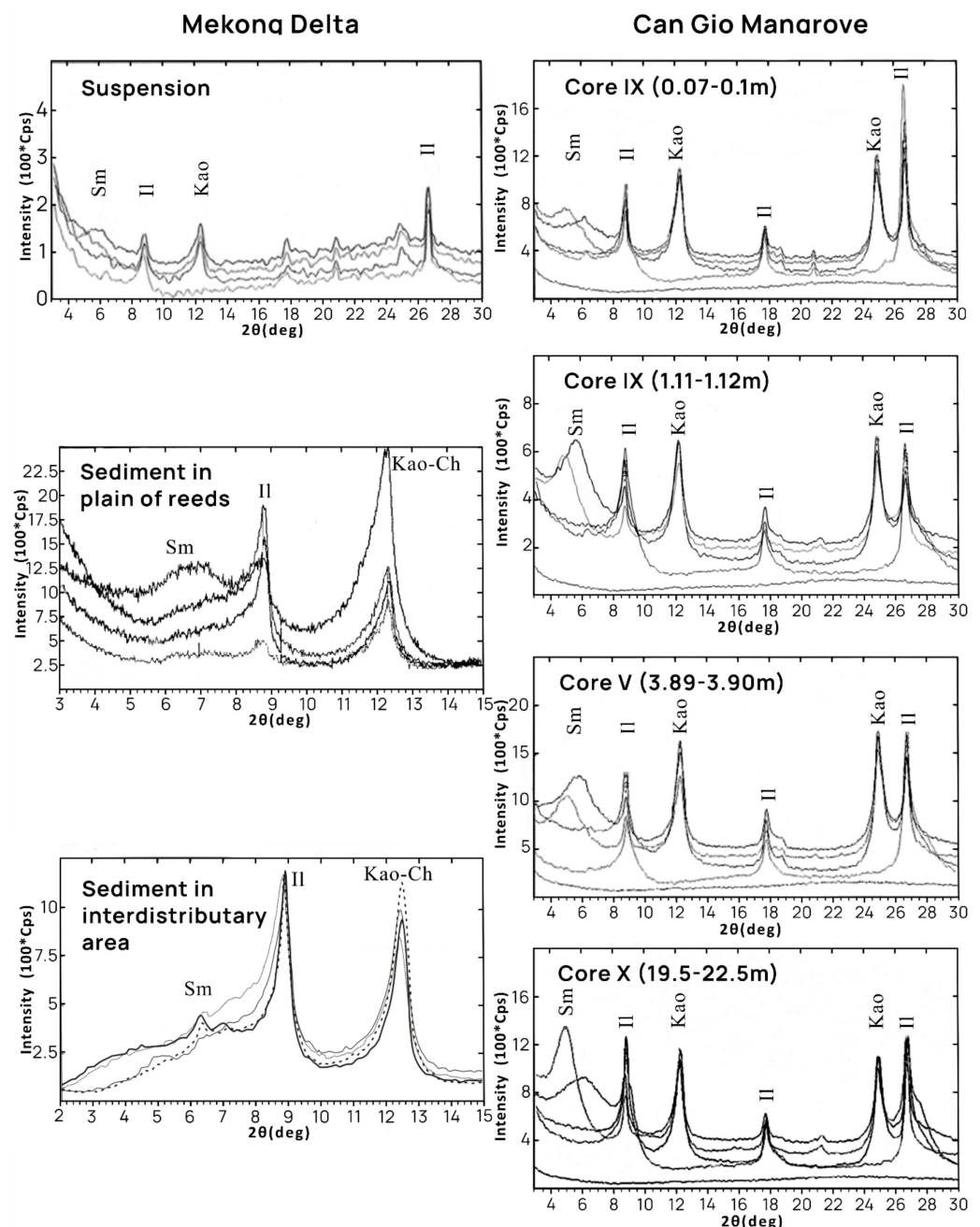


**Figure 6.** Representative X-ray diffractions showing the different proportion of clay minerals from sediments of CG (this study) and from MKD sediments [63]. Sm—smectite; Ch—Chlorite; Kao—Kaolinite; II—Illite.

**Table 1.** Results of radiocarbon dating.

Lab Code	Core	Sample Depth (cm)	Sample Material	Position	Recovery Depth (cm)	Conventional <sup>14</sup> C Age (Years)	Calibrated Age (2 Sigma) Years
KIA 28516	Core V	115	Mangrove fragment	10°25'2.97" N 106°52'50.87" E	390	525 ± 30 BP	185 ± 80 BP
KIA 28517	Core V	376	Mangrove fragment	10°25'2.97" N 106°52'50.87" E	390	535 ± 25 BP	195 ± 76 BP
KIA 33203	Core VI	30	Shell	10°25'04.28" N 106°52'48.58" E	353	720 ± 25 BP	378 ± 62 BP
KIA 28518	Core VI	322	Shell fragment	10°25'04.28" N 106°52'48.58" E	353	825 ± 25 BP	474 ± 48 BP
KIA 33205	Core IX	62	Shell fragment	10°22'30.39" N 106°52'05.72" E	123	375 ± 30 BP	<144 ± 80 BP
KIA 33206	Core IX	81	Shell fragment	10°22'30.39" N 106°52'05.72" E	123	4820 ± 35 BP	5148 ± 102 BP
KIA 28515	Core IX	107	Shell fragment	10°22'30.39" N 106°52'05.72" E	123	4845 ± 35 BP	5173 ± 100 BP
KIA 45568	Core 130508-C1	10–12	Organic material	10°26.14.04" N 106°57.22.14" E	97	3240 ± 45 BP	3446 ± 71 BP

Based on the variation of the biological index  $I_c$  in the sediment of cores V and VI, we detected a comparative stability of marine influence versus continental influence during a relatively rapid accretion that occurred until ca. 0.2 ka BP (Figure 7). Later, a dramatic change in the environmental conditions with the reversal to continental influence appeared, which was becoming dominant;  $I_c$  is nearly 1, showing a high level of confinement in the upper part of core V after ca. 0.2 ka BP, or a dominance of the C-group. The dominance of this foraminifera group, which is characteristic of brackish water environments or in mangroves [61], leads to the interpretation that it was a back-barrier lagoonal environment, which has been established in accordance with the deposition of the sandy beach, as shown in Figure 3. Subsequently, a colonization of mangroves on the extended shallow intertidal flats occurred. This means that the Dong Tranh river mouth (Figure 3) could have been larger or more open prior to the formation of the current sandy beach. On the other hand, the central mangrove patch was much narrower in the past. Figure 7 shows the interpretation of the depositional environment within the sampling sites in the Dong Tranh river mouth. Accordingly, a transition evolving from a sub-littoral zone to a back-barrier lagoon and then an emergence of mangroves since 0.2 ka BP occurred.

Based on the chronological record vs. depth and the seismic profile (Figure 5), the deposition is limited around the location of core IX and station 130508-C1 in the outer part of the Dong Tranh channel and in Ganh Rai Bay (Figure 1). The amount of sediment discharged by the river seems to be poor. On the other hand, a high sedimentation occurred along the western side of the mangrove patch at the sites of cores V and VI (Figure 3).

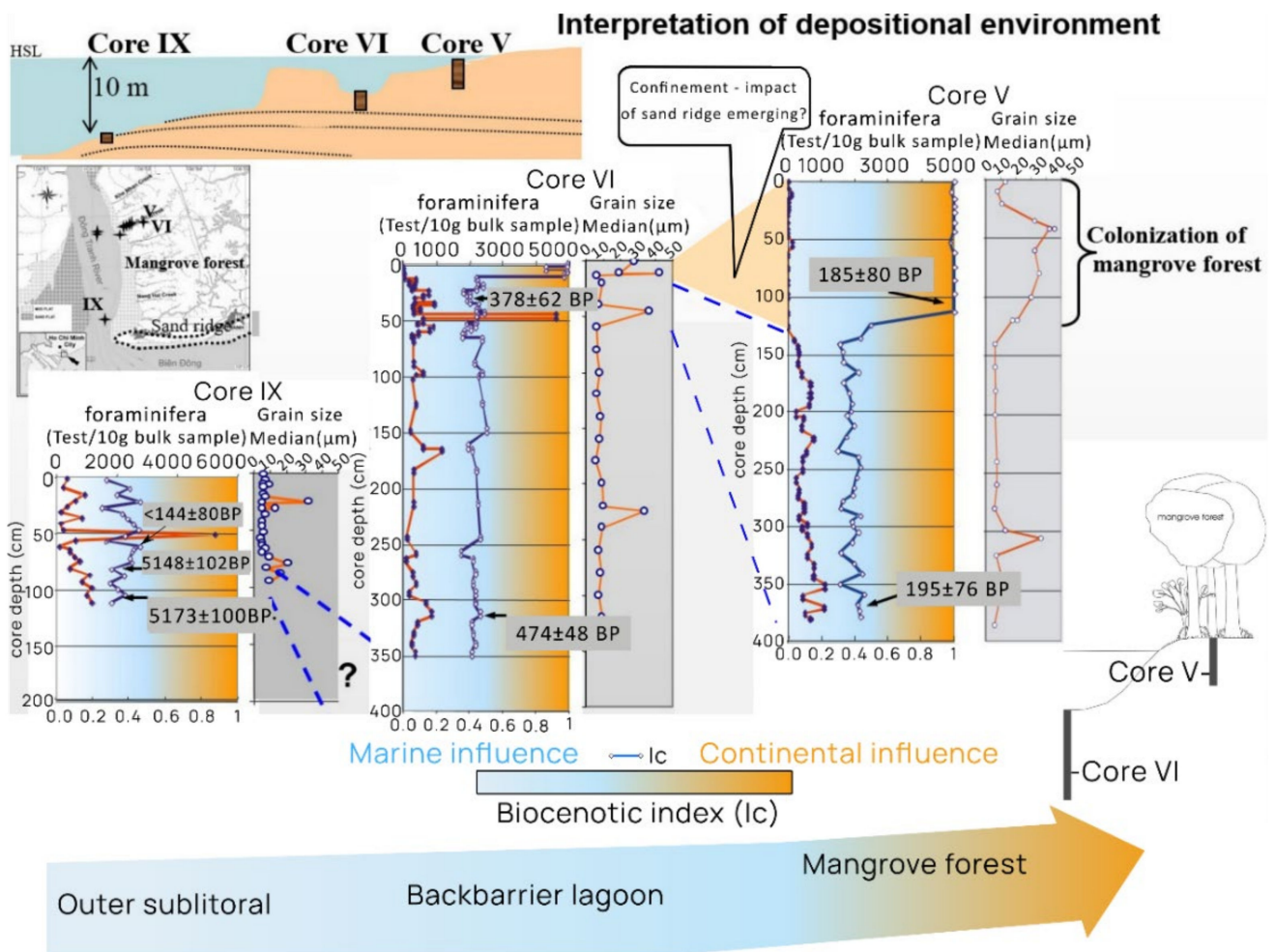


**Figure 7.** Development of the depositional environment in the study area since the Late Holocene. Colors on the chart showing the distribution of foraminifera: orange line—density of foraminifera; blue line—variability of biocenotic index (Ic).

### 3.2. Domains of Abrasion and Accumulation along the Coastline of Can Gio

Figure 8 shows a smooth coastline at sector I representing a dominantly dissipative environment that is characterized by large mudflats. Along sector II, the formation of a 1–2 m-high active cliff indicates intense abrasion and coastal retreat with a rate of a few meters/year [48]. The sandy coast of sector III has been strongly eroded in the past. Therefore, it was recently entirely protected by a dyke and groins. The sandy ridges extend parallelly to the coast for a distance of about 10.5 km. The sand, which is concentrated on the beach and ridges, is fine and mixed with organic fragments. The shape and crest of the sand dune shows that winds from the northeast during the dry season (Figure 2) are the main driving force for the sand movement in east-west direction, indicated by the downwind sand accumulation observed behind grass clusters. Luv-accumulation at the eastern side of the groins and lee-side erosion on the western side (Figure 8) indicate the same transport direction in the nearshore environment. The disposition of sand bodies is also shown in topographic maps.

Notably, storms appear irregularly at the end of the year. Sometimes, a cold surge induced by the northeast monsoon forces their tracks to divert to lower latitudes and causing landfall from the east side to the CG and the MRD. These tropical storms always cause severe storm surges and coastal flooding. In fact, during the last decades, two major storms, Linda in December 1997 and Durian in December 2006, swept over CG for hours, partly causing a water surge, which collapsed in the forest.

Our subsidence monitoring stations were implanted later in 2010 (Figure 1, SET-MH technique) at a clear cutting in the forest, which was created by the track of typhoon Durian. The results obtained show a really high rate of land subsidence with nearly 4 cm/year, lasting up to 10 years after the event. After that time, the rate decreased gradually. However, it was significantly lower in the surrounding forest than in the forest gap, where mangroves have recovered naturally. Thus, besides the commonly known consequences such as coastal abrasion, storm-related damages cause also indirect medium-term effects, modifying and lowering the ground and resulting in frequent coastal flooding.



**Figure 8.** The coastal sectors—II and III around Can Gio represent the different status of the coastline; accumulation at sector I, erosion at sector II and longshore sediment transport and shore protection at sector III. The subpictures (a,b) represent an overview (a) and a cutout (b).

### 3.3. Modern Trend: Coastal Abrasion and Accumulation

The observed and pronounced erosion along the coastline is driven by natural factors and human intervention such as shore protection and/or dredging operations in the navigation channels. Erosion is strong along those shorelines, which are exposed directly to the sea and to the fetch length of Ganh Rai Bay during the NE monsoon. Besides the western coast of Ganh Rai Bay and the southern coast of sectors II and III (Figure 8), there are other areas that are the most affected by coastal abrasion, such as the mouths of the major distributaries Long Tau, Dong Tranh and Soai Rap (for locations, see Figure 1). As the wind influence of the NE monsoon approaching from the sea is more intense compared to the SW

monsoon and the water level is generally higher during the NE monsoon (Figure 2) [12,48], both usually enhance the amplitude of the high tide surge, introducing more stress on the shoreline. Therefore, compared to the western areas, small landslides and cliffs are spread more intensively along the banks of the tidal channels that are exposed towards the east. In addition, a relatively slow delay of tide propagation to the west occurs if we compare the data recorded at Vung Tau with the coastal gauges along the eastern coast of the MRD [64]. As a result, a significant amount of suspended material is diverted in this direction. In addition, abnormally high sedimentations were recorded at the land subsidence monitoring station (Figure 9; for locations, see Figure 1). This accumulation appeared coincidentally with the implementation of dredging operations for a new navigation channel inside the Soai Rap estuary, which were carried out from 2011 to 2014. When the dredging operations were completed, the sedimentation rate gradually returned to its former value (Figure 9).

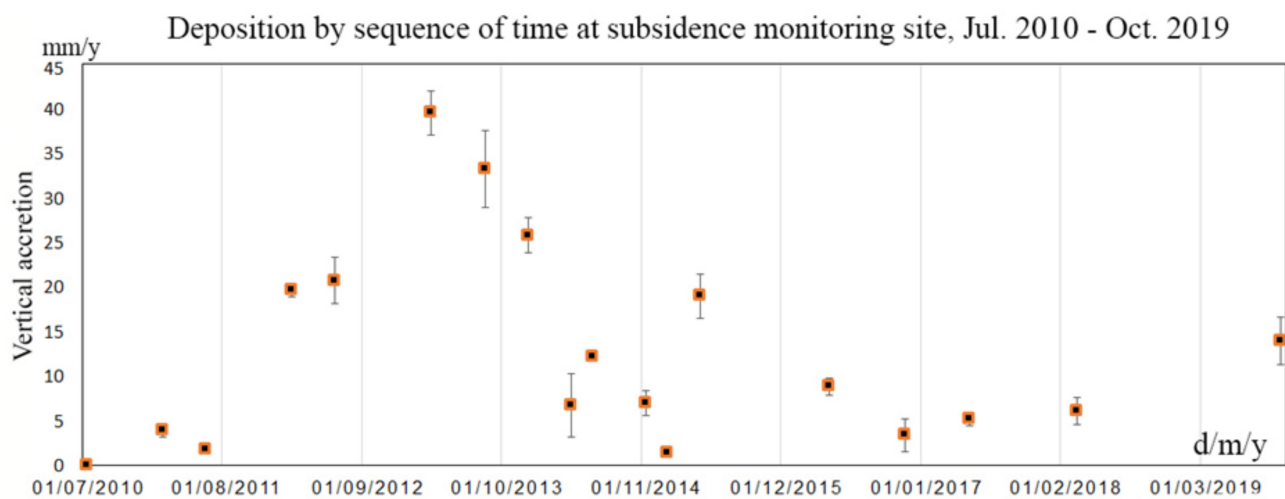


**Figure 9.** Short-term deposition rate recorded at the subsidence monitoring site, since July 2010 (for the location of the monitoring site, see Figure 1).

As the locations of dredging and subsidence monitoring are spatially relatively close together (Figure 1), resuspended sediment from the Soai Rap channel was able to be pushed into the adjacent mangrove forest by tides and, therefore, could contribute to additional accretion. Moreover, many small tidal creeks connecting to the Soai Rap estuary became locally blocked and were impenetrable.

#### 4. Discussion

##### 4.1. Development of the Sai Gon-Dong Nai River Delta

Regarding the location of CG, it was thought that this low land is a marginal basin of the MRD [65] and that it formed from the southwest to the northeast direction with a delta evolution during the last 2.6 ka BP and covered almost the same area as it currently does by 0.4 ka BP [27]; however, our interpretation presents another picture. The SG-DNR discharges into a relatively low energy environment inside a semi-open bay, which is about 30 m deep. Further inland, the Pleistocene basement was discovered at a 27 m depth in core CG-2 [28]. This bay is limited from the northeast by the terrace of a Pleistocene basement and it is blocked from the sea by a shoal that also belongs to the Pleistocene basement. This shoal extends around the current coast. Its roof is submerged at a depth of 14 m in core CG-1 [28], at 4.6 m in one core implanted on the outer beach [35], at a depth of 14 m near the confluence of the Soai Rap and Vaico distributaries (pers. communication from the Chief Engineer of the Soai Rap dredging project) and at about 13 m depth in the Long Tau River (Figure 1). Based on an age model, Collins et al. [28] believe that a highly aggradational accumulation occurred and formed a shallow substrate since 6.0 ka during the regional sea-level highstand [66] and the subsequent sea level drop. At

that time, monsoon activities were still relatively strong [67], and it was possible that the existing strong coastal hydrodynamic affected the sediment's accumulation. However, the mountain range and rocky headland Vung Tau are likewise a natural shield for reducing the attack of strong winds and waves from NE, retaining relatively calm conditions in the inner part of CG.

Accordingly, the accretion of deposits (delta front and prodelta) had already established a shallow subtidal environment about 3.5 ka BP, just below the current most advanced seaward shoreline [28].

The subtidal and intertidal environments probably advanced towards the sea from the current shoreline, because these deposits and a peat layer were found below the modern sand beach in boreholes (Figure 1) implanted in the outer part of the beach [35]. Furthermore, the shallow Pleistocene basement existing beneath the present coast, even at a 4.6 m core depth in one core implanted on the outer beach [35] and farther offshore in the seismic profile (Figure 5), also supports this progradation. Consequently, the rapid progradation occurred after 3.5 ka, corresponding to the  $^{14}\text{C}$  ages obtained from core CG-1 [28]. At that time, the position of the delta front and prodelta of the MRD was still running far inland, about 40–50 km distant from its current shoreline [39].

Besides the geological characteristics, a hydrological disparity in the pristine water courses in CG, its adjacent area and in the distributaries of the Mekong River was already reported [68]. Accordingly, the impact of a tide-dominated water regime in the Can Gio, Soai Rap and Vai Co rivers was significant farther to the west than in the northeastern-most distributaries Cua Tieu and Cua Dai of the Mekong River (for locations of distributaries, see Figure 10). The water discharge through these courses was estimated from none to 6% of the entire Mekong River's flow in the dry season [69]. In the rainy season, the flow of Soai Rap and Vai Co rivers impedes the transfer of the Mekong River discharge through these distributaries to the east. The fluvial regime controlled the western distributaries of the Mekong River. Thus, this disparity must have influenced differently the transfer and distribution of river-solid discharge of the SG-DNR and the Mekong Rivers in the coastal water in Can Gio and the northeastern part of the MRD.

Although the four clay minerals, Illite, Kaolinite, Smectite and Chlorite, are always present in the sediment of CG and the MRD, the proportions in their clay assemblage are different (Figure 6). There is a pronounced abundance of Smectite in CG, accounting for more than 30%, but this clay mineral appears only as traces in the suspension load and the sediments from the Mekong River [63]. Smectite is a result of weathering of basic rocks [62], such as the Quaternary alkaline plateau basalts widely present in the Dong Nai River catchment (Figure 10). These alkaline basalts are regarded as the source for the high content of this clay mineral in the sediments. Apparently, CG region receives alluvial materials deriving from another source that is mostly from the Dong Nai River catchment and separate of those from the Mekong River. However, the boundary between these two large sedimentary systems has not yet been clearly demarcated.

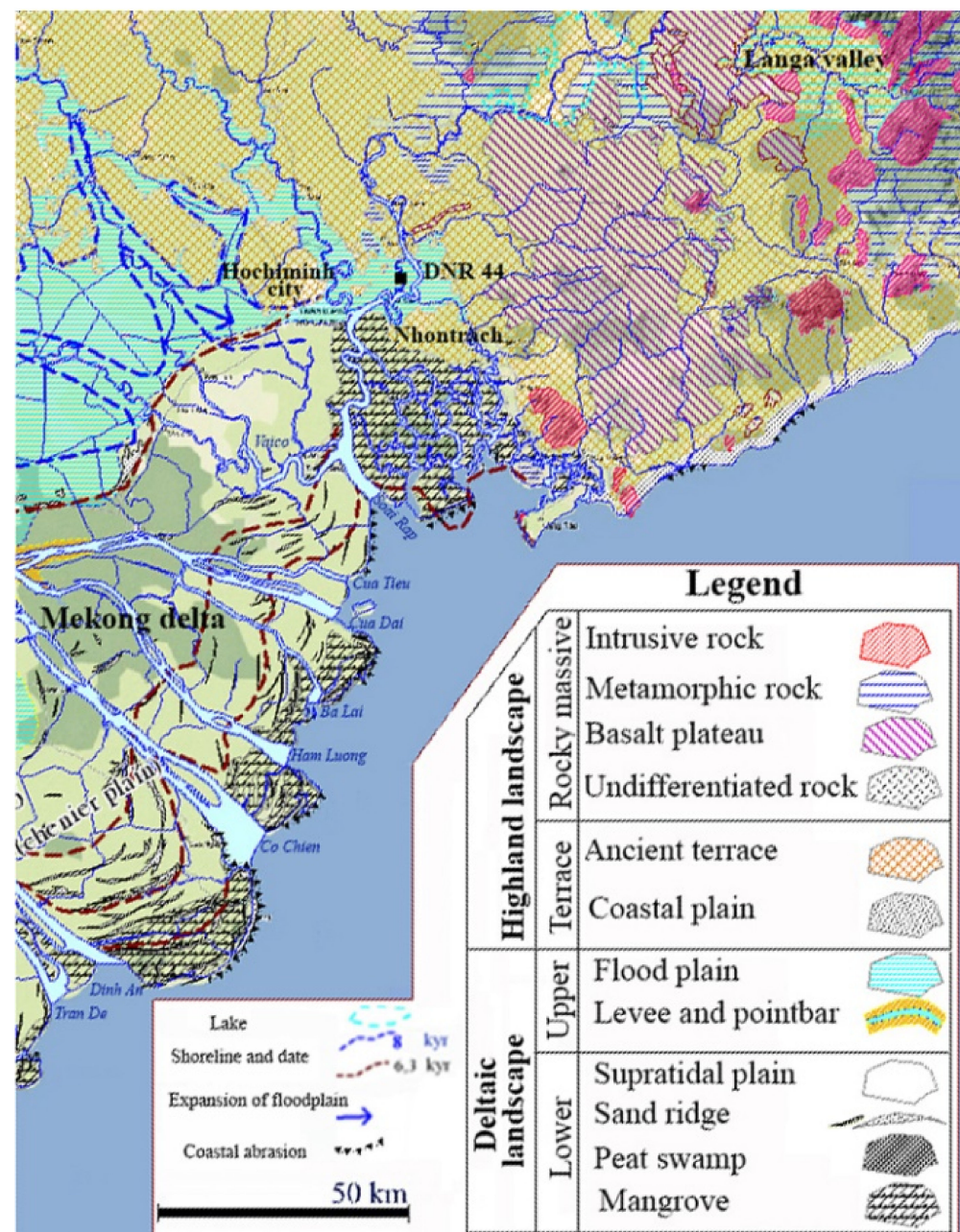


**Figure 10.** The main geological formations in the catchment of the SG-DNR and the adjacent area. The location of core site DNR 44 [27] is shown. The background map is extracted from [70] (Le et. al., 2017) with some added notes in the English language.

As all modern deltas, similarly to the MRD, started to form during the stable sea-level conditions from 7 to 8 ka BP [71], the formation of the estuarine deposits of SG-DNR system certainly occurred at the same time. Similarly, a landward limit of highstand systems tract (HST) was recorded through the sediment column at the DNR 44 site [27] located about 50 km inland from the present coastline (Figure 10). At this site, beneath about 0.6 m of a modern fluvial deposit, a depositional architecture typical for the transgression and HST is present. There is a 10 cm-thick peat layer overlying a thin mangrove organic deposit, with the age bracketed with the two dates 6.63 ka cal. BP at a depth of 84 cm and 7.490 ka cal. BP at a depth of 240 cm, respectively. Below this organic deposit, a thin layer of brownish grey loam of about 0.2 m thickness exists, followed by a stiff Pleistocene substratum. This evidence suggests that the apex of the SG-DNR tide-dominated delta may be demarcated at the location, which is squeezed between two high terraces built up

by Pleistocene deposits, located downtown of HCMC and Nhontrach town (Figure 10). Thus, the deposits of the SG-DN river system in a semi-open bay started its development around 7.5 ka BP, which is quite close to the initiation of the MRD nearby [72]. In terms of the abundance of sediment as an important source for the rapid expansion of the mangrove patches, it is highly probable that intense soil erosion, as a result of the acceleration of land reclamation by extensive human occupation in the river catchment, is the reason. In this catchment area, a continuous prehistoric settlement from the Stone Age (Neolithic) to Bronze–Iron Age cultures and the subsequent Funan culture (ca. 3–2 ka BP), a primitive maritime state in the region as recognized in the recent archaeological discovery, was observed [72,73]. Despite the fact that the central patch of mangrove stretched far towards the sea in the N–S direction (Figure 11), it was likely restricted in a narrow form. However, the later formation of a coastal sand ridge plays a certain role in the lateral expansion of the mangrove forest. The relative low energy environment existing behind the sand ridge supported a rapid accretion of prodelta deposits and then a lateral expansion of mangrove forests that occurred since the last millennium and about 0.5 ka, respectively, as observed at the two core sites of VI and V (Figure 7).

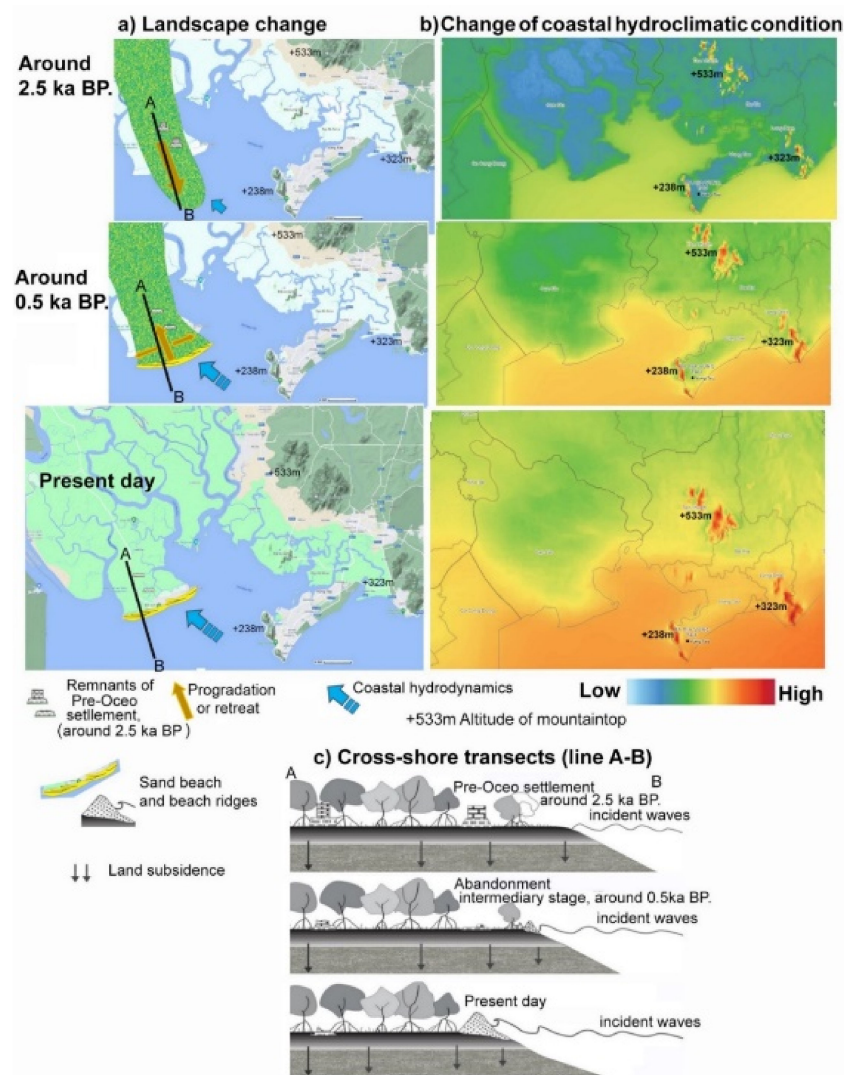


Figure 11. The development of the central mangrove patch at the CG area for the last 2000 years.

#### 4.2. Formation of the Coastal Sand Ridge

In terms of wave energy, mangrove species grow best in sheltered depositional environments with low-energy input by waves and currents [74]. If mangroves are considered as dissipative environments suitable for sediment accumulation [75], a complex of long sand ridges and a sandy beach, existing along the coast of sector III (Figure 8), must have clearly formed in a contrary depositional condition. The coexistence of the different types of energetic coasts can be a result of a historical interaction between the sea and the land as it is recorded from other coastal zones [76].

Indicated by a pair of Quartz OSL dating techniques, it is believed that this coastal sand ridge formed about 3.2 ka BP [28]. However, looking at the nearby coast along the western bank of the Soai Rap estuary (Figure 1), the large sand-ridge plain of the MRD exists, and most sand ridges here formed from 2 ka up until now [77].

In addition, the results of archaeological investigations provide valuable information related to the complex of coastal sand ridges. Many archaeological sites, which have been already discovered (Figure 1) and which belong to the pre-Oc Eo culture [78], are concentrated here. This was the first stage of the famous Funan culture, which existed in the region until 7th century AD [50]. Remarkably, no sites have been found on the sand ridge, although its high altitude would have rendered it a safe location against coastal flooding. Moreover, in these low-lying environments, the ancient communities had to carry red soil (basaltic soil) far from the outside of the Can Gio mangrove to build up their residential foundations, as discovered under the Phet mound [16]. In particular, many ceramic objects and jar-tombs have been discovered here, and the burial objects at the two sites Cavo and Phet (Figure 1) have radiocarbon ages from  $2.4 \pm 0.48$  to  $2.1 \pm 0.50$  ka BP, respectively [16].

Obviously, it is not reasonable if there were already the high sand ridges existing, but the ancient communities carried red soil from afar to build up these mounds on tide-flooded lands in the mangroves. Therefore, it is inferred that these previously uninhabited sand ridges surely did not exist before or did not exist simultaneously with foundations such as the Phet mound, estimated around 2.1 ka BP [16], and after the abandonment of the pre-Oc Eo culture settlement or later than the first century BCE (before the common area). Thus, the appearance of these sand ridges was a termination of the longitudinal expansion and marked a great change in coastal hydrodynamics from about 2 ka BP to the present in the coastal area of the CG.

Regarding coastal hydrodynamics, the seasonal characteristics of wind, wave and tidal conditions are demonstrated in Figure 2. Apparently, the intensity of these factors increases in the winter season in response to the cold air blowing from NE under the variation of the EAM. Concerning regional climatic variations, the EAM declined during the middle Holocene and gradually recovered its power over Southeast Asia again in the last 2 ka [66,78]. Furthermore, the impact of the monsoon on the geomorphology and the sediment of a mesotidal beach on the Mekong River was previously documented [79].

In addition, the mountain range and rocky headland of Vung Tau are likewise a natural shield to promote the seaward extension of CG. Once the central mangrove patch extended seaward from the protected area created by this shield, its head underwent destructive actions, when the hydrodynamic conditions increased. As a result, coastal recession started to occur along with the formation of sand ridges.

The large amounts of sand providing the growth of the sand ridge must have been transported from outside because its structure is different from the common fine-grained sediments deposited below the CG mangrove. In fact, a longshore sand transport from the northeastern coast, farther from Vung Tau Cape, can be its source. In this adjacent coast, a dominant down-drift accumulation of sand in NE-SW directions is recorded and is related to the prevailing wind during the EA winter monsoon activity [80,81].

#### 4.3. Geomorphological Evolution of CG

The SG-DNR discharges into a relatively low-energy environment inside a semi-open bay. It started to form its own tide-dominated delta during the regional Holocene sea-level

highstand about 6.7–5.0 ka BP east of HCMC. This condition was favorable for a rapid accretion of the prodelta deposits, as observed in cores CG-1 and CG-2 [28], and then for the colonization of mangroves.

Later, along with weakening oceanic forces due to a decrease in the EAM, the head of the central mangrove patch extended further seaward during the early Late Holocene, even farther from the present shoreline. At this time, the settlement of the pre-Oc Eo community in the second half of the first millennium BC occurred. After encroaching its distant position about two thousand years ago, this foreland gradually experienced more destructive actions from the sea.

Furthermore, our interpretation about the recent development of the entire CG area is modeled and shown in Figure 11. The evolution of the central mangrove patch is illustrated mainly with respect to the change of coastal hydrodynamics caused by the enhancement of the EAM, starting since the last two millennia [67]. Thus, the CG area began to shift backwards due to coastal erosion. As a result, the mangrove patch in the more exposed areas collapsed and was buried under the new onshore deposition of sand, as observed in the outer current beach.

Along with the coastal recession, the erosion in the surf zone provides a considerable amount of material to promote increasing sediment relocations inside the mangroves. The relative secluded locations and back-barrier conditions behind the sand ridge and farther inland are also suitable locations for sediment deposition. This occurs intensively, in particular, in the western part of the central patch of the mangrove, as observed through the high rate of sedimentation measured at core sites V and VI (Figure 7) and based on  $^{210}\text{Pb}$  activities obtained from short cores taken at the sites CG-01, CG-02, CG-03 and TV-05 [82] (see Figure 1).

In addition, on a shorter timescale, the implementation of dredging operations in Long Tau and Soai Rap rivers additionally provided a large volume of suspensions deposited inside the mangrove forest and filling up even some tidal creeks. One result of these processes is obvious by observing a short increase in sedimentation, demonstrated in Figure 8. Today, CG is experiencing an increased impact of marine abrasion, which is mostly concentrated in the eastern part in sectors II and III [33,34] (Figure 8). Moreover, CG might experience additional impacts in the future due to development projects such as the embankment of the coastal flood control for HCMC involving a long sea dyke stretching from Vung Tau cape to the MK delta coast, the construction of a seaport or the construction of a new coastal city on the current sand ridge.

## 5. Conclusions

Abundant sediment supplies from the SG-DNR basin supported the initiation and evolution of the CG tide-dominated delta since about 8 ka BP. The development of the delta occurred due to the interplay of specific local factors such as geological structures, including the characteristics of the Pleistocene basement, the location of Vung Tau rocky headland and the variation of the EAM on the regional scale. This area developed independently from the MRD and became a favorable environment for mangroves to develop.

After a period of rapid seaward progradation, until about 1 ka BP, the protruding mangrove area began a new process of change, with the increasing coastal hydrodynamic impact and an intense erosion under the pronounced strong activity of the EAM. As a result, the coastline was continuously pushed landward. Along with this process, a complex of unique sand ridges formed on the current protruding coast in the southeast after first century BCE. At the same time, the eroded sediment is entrained and re-deposited back into the mangroves, supporting a lateral expansion of mangrove patches to the west within tidal channels. Currently, in addition to these actions, CG mangrove environments are facing large impacts caused by human intervention.

**Author Contributions:** Conceptualization, T.X.L. and K.S.; methodology, T.X.L., K.S., L.T.B., T.C.N. and D.U.; formal analysis, T.X.L., L.T.B. and K.S.; investigation, K.S., T.X.L. and T.C.N.; resources, K.S. and T.X.L.; data curation, K.S.; writing—original draft preparation, T.X.L. and K.S.; writing—review and editing, T.X.L. and K.S.; visualization, T.X.L., T.C.N. and D.U.; project administration, K.S.; funding acquisition, K.S. and T.X.L. All authors have read and agreed to the published version of the manuscript.

**Funding:** This research was funded by Deutsche Forschungsgemeinschaft (DFG) grant No. SCHW 572/8-1, 572/8-2 and 572/8-3 and the Ministry of Science and Technology of Vietnam (MOST).

**Institutional Review Board Statement:** Not applicable.

**Informed Consent Statement:** Not applicable.

**Data Availability Statement:** Not applicable.

**Acknowledgments:** Funding for this study was provided by DFG (German Research Foundation) and MOST (Ministry of Science and Technology, Vietnam) throughout the joint German-Vietnamese research project “Land-ocean-atmospheric interaction in the coastal zone of Southern Vietnam”; subproject “Sediment Dynamics in Mangrove Areas—SEDYMAN I–II”, grant number SCHW 572/8-1, 572/8-2 and 578/8-3.

**Conflicts of Interest:** The authors declare no conflict of interest. The funders had no role in the design of the study; in the collection, analyses, or interpretation of data; in the writing of the manuscript; or in the decision to publish the result.

## References

1. Wright, L.D. Sediment Transport and Deposition at River Mouths: A Synthesis. *GSA Bull.* **1977**, *88*, 857–868. [CrossRef]
2. Fagherazzi, S.; Edmonds, D.A.; Nardin, W.; Leonardi, N.; Canestrelli, A.; Falcini, F.; Jerolmack, D.J.; Mariotti, G.; Rowland, J.C.; Slingerland, R.L. Dynamics of River Mouth Deposits. *Rev. Geophys.* **2015**, *53*, 642–672. [CrossRef]
3. Dalrymple, R.W.; Choi, K. Morphologic and Facies Trends through the Fluvial-Marine Transition in Tide-Dominated Depositional Systems: A Schematic Framework for Environmental and Sequence-Stratigraphic Interpretation. *Earth Sci. Rev.* **2007**, *81*, 135–174. [CrossRef]
4. Smith, T.J., III. Forest Structure. In *Tropical Mangrove Ecosystems*; American Geophysical Union: Washington, DC, USA, 1992; p. 329.
5. Mazda, Y.; Wolanski, E.; Ridd, P. *The Role of Physical Processes in Mangrove Environments*; Terrapub: Tokyo, Japan, 2007; p. 598.
6. Woodroffe, C.D.; Rogers, K.; McKee, K.L.; Lovelock, C.E.; Mendelsohn, I.A.; Saintilan, N. Mangrove Sedimentation and Response to Relative Sea-Level Rise. *Ann. Rev. Mar. Sci.* **2016**, *8*, 243–266. [CrossRef] [PubMed]
7. Hanebuth, T.J.J.; Voris, H.K.; Yokoyama, Y.; Saito, Y.; Okuno, J. Formation and Fate of Sedimentary Depocentres on Southeast Asia’s Sunda Shelf over the Past Sea-Level Cycle and Biogeographic Implications. *Earth Sci. Rev.* **2011**, *104*, 92–110. [CrossRef]
8. Statterger, K.; Tjallingii, R.; Saito, Y.; Michelli, M.; Trung Thanh, N.; Wetzel, A. Mid to Late Holocene Sea-Level Reconstruction of Southeast Vietnam Using Beachrock and Beach-Ridge Deposits. *Glob. Planet. Change* **2013**, *110*, 214–222. [CrossRef]
9. Le, D.T.; Tran, T.K.O.; Cat, V.T.; Nguyen, D.Q. *Can Gio Mangrove Biosphere Reserve*; Agriculture Publisher: Ho Chi Minh City, Vietnam, 2002.
10. Chan, T.H.; Cohen, M. *Studies in Can Gio Mangrove Biosphere Reserve, Ho Chi Minh City, Viet Nam*; Mangrove Ecosystems Technical Reports No. 6; International Society for Mangrove Ecosystems (ISME): Okinawa, Japan, 2014; 63p.
11. Kuenzer, C.; Vo, Q.T. Assessing the Ecosystem Services Value of Can Gio Mangrove Biosphere Reserve: Combining Earth-Observation- and Household-Survey-Based Analyses. *Appl. Geogr.* **2013**, *45*, 167–184. [CrossRef]
12. Schwarzer, K.; Nguyen, C.T.; Ricklefs, K. Sediment Re-Deposition in the Mangrove Environment of Can Gio, Saigon River Estuary (Vietnam). *J. Coast. Res.* **2016**, *75*, 138–142. [CrossRef]
13. Costa-Böddeker, S.; Hoelzmann, P.; Le, X.T.; Hoang, D.H.; Nguyen, H.A.; Richter, O.; Schwalb, A. Ecological Risk Assessment of a Coastal Zone in Southern Vietnam: Spatial Distribution and Content of Heavy Metals in Water and Surface Sediments of the Thi Vai Estuary and Can Gio Mangrove Forest. *Mar. Pollut. Bull.* **2017**, *114*, 1141–1151. [CrossRef]
14. Costa-Böddeker, S.; Le, X.T.; Hoelzmann, P.; de Stigter, H.C.; van Gaever, P.; Hoang, D.H.; Smol, J.P.; Schwalb, A. Heavy Metal Pollution in a Reforested Mangrove Ecosystem (Can Gio Biosphere Reserve, Southern Vietnam): Effects of Natural and Anthropogenic Stressors over a Thirty-Year History. *Sci. Total Environ.* **2020**, *716*, 137035. [CrossRef]
15. Le Nguyen, H.T.; Vo Luong, H.P. Erosion and Deposition Processes from Field Experiments of Hydrodynamics in the Coastal Mangrove Area of Can Gio, Vietnam. *Oceanologia* **2019**, *61*, 252–264. [CrossRef]
16. Nguyen, T.H. Overview of Archaeological Relics of the “Pre-Oc Eo” Period in the Southern Region. Vietnam National Museum of History. 2017. Available online: <https://baotanglichsu.vn/vi/Articles/3127/62082/khai-quat-ve-cac-di-tich-khao-co-hoc-thuoc-giai-djoan-tien-oc-eo-o-nam-bo.html> (accessed on 1 January 2018). (In Vietnamese).
17. Spalding, M.; Kainuma, M.; Collins, L. *World Atlas of Mangroves 2010*; Routledge: London, UK, 2010.

18. Vo, T.; Kuenzer, C. *Can Gio Mangrove Biosphere Reserve Evaluation of Current Status, Dynamics, and Ecosystem Services, 2012*; IUCN: Gland, Switzerland, 2013.
19. Anthony, E.J.; Brunier, G.; Besset, M.; Goichot, M.; Dussouillez, P.; Nguyen, V.L. Linking Rapid Erosion of the Mekong River Delta to Human Activities. *Sci. Rep.* **2015**, *5*, 14745. [[CrossRef](#)] [[PubMed](#)]
20. Coleman, J.M.; Roberts, H.H. Deltaic Coastal Wetlands. In *Coastal Lowlands*; van der Linden, W.J.M., Cloetingh, S.A.P.L., Kaasschieter, J.P.K., van de Graaff, W.J.E., Vandenbergh, J., van der Gun, J.A.M., Eds.; Springer: Dordrecht, The Netherlands, 1989; pp. 1–24, ISBN 978-90-481-4038-1.
21. Milliman, J.D.; Farnsworth, K.L. *River Discharge to the Coastal Ocean*; Cambridge University Press: Cambridge, UK, 2011. ISBN 9780511781247.
22. Wang, J.J.; Lu, X.X.; Kumm, M. Sediment Load Estimates and Variations in the Lower Mekong River. *River Res. Appl.* **2011**, *27*, 33–46. [[CrossRef](#)]
23. Debenay, J.-P.; Bui, T.L. Foraminiferal Assemblages and the Confinement Index as Tools for Assessment of Saline Intrusion and Human Impact in the Mekong Delta and Neighbouring Areas (Vietnam). *Rev. Micropaléontol.* **2006**, *49*, 74–85. [[CrossRef](#)]
24. Dijkma, R.; Van Loon, A.; van Mensvoort, M.; Huijgevoort, M.; te Brake, B. An Extended Hydrological Classification for Mangrove Rehabilitation Projects: A Case Study in Vietnam. In *Tropical Deltas and Coastal Zones—Food Production, Communities and Environment at the Land-Water Interface*; Hoanh, C.T., Szuster, B.W., Kam, S.-P., Ismail, A.M., Noble, A.D., Eds.; CABI: Wallingford, UK, 2010; pp. 384–397. ISBN 978 1 84593 618 1.
25. Lovelock, C.E.; Cahoon, D.R.; Friess, D.A.; Guntenspergen, G.R.; Krauss, K.W.; Reef, R.; Rogers, K.; Saunders, M.L.; Sidik, F.; Swales, A.; et al. The Vulnerability of Indo-Pacific Mangrove Forests to Sea-Level Rise. *Nature* **2015**, *526*, 559–563. [[CrossRef](#)]
26. Costa-Böddeker, S.; Le, X.T.; Hoelzmann, P.; Stigter, H.; Gaever, P.; Hoang, D.H.; Schwab, A. The Hidden Threat of Heavy Metal Pollution in High Sedimentation and Highly Dynamic Environment: Assessment of Metal Accumulation Rates in the Thi Vai Estuary, Southern Vietnam. *Environ. Pollut.* **2018**, *242*, 348–356. [[CrossRef](#)]
27. Fujimoto, K.; Masatomo, U.; Nguyen, V.L.; Ta, T.K.O.; Kawase, K.; Huynh, D.H.; Nakamura, T. Geomorphological Evolution and Mangrove Habitat Dynamics Related to Holocene Sea-Level Changes in the Northern Mekong River Delta and the Dong Nai River Delta, Southern Vietnam. In *River Deltas: Types, Structures and Ecology*; Schmidt, P.E., Ed.; Nova Science Publishers Inc.: Hauppauge, NY, USA, 2011; pp. 125–141.
28. Collins, D.S.; Nguyen, V.L.; Ta, T.K.O.; Mao, L.; Ishii, Y.; Kitagawa, H.; Nakashima, R.; Vo, T.H.Q.; Tamura, T. Sedimentary Evolution of a Delta-Margin Mangrove in Can Gio, Northeastern Mekong River Delta, Vietnam. *Mar. Geol.* **2021**, *433*, 106417. [[CrossRef](#)]
29. Nguyen, T.N.T.; Némery, J.; Gratiot, N.; Strady, E.; Tran, Q.V.; Nguyen, T.A.; Aimé, J.; Peyne, A. Nutrient Dynamics and Eutrophication Assessment in the Tropical River System of Saigon-Dongnai (Southern Vietnam). *Sci. Total Environ.* **2019**, *653*, 370–383. [[CrossRef](#)]
30. Szczuciński, W.; Jagodziński, R.; Hanebuth, T.J.J.; Statterger, K.; Wetzel, A.; Mitreğa, M.; Unverricht, D.; Van Phach, P. Modern Sedimentation and Sediment Dispersal Pattern on the Continental Shelf off the Mekong River Delta, South China Sea. *Glob. Planet. Change* **2013**, *110*, 195–213. [[CrossRef](#)]
31. Nguyen, T.T.; Statterger, K.; Unverricht, D.; Nittrouer, C.; Phung, V.P.; Liu, P.; DeMaster, D.; Bui, V.D.; Le, D.A.; Mai, D.D. Surface Sediment Grain-Size Distribution and Sediment Transport in the Subaqueous Mekong Delta, Vietnam. *Vietnam. J. Earth Sci.* **2017**, *39*, 193–209. [[CrossRef](#)]
32. Gugliotta, M.; Saito, Y.; Ta, T.K.O.; Nguyen, V.L.; Uehara, K.; Tamura, T.; Nakashima, R.; Lieu, K.P. Sediment Distribution along the Fluvial to Marine Transition Zone of the Dong Nai River System, Southern Vietnam. *Mar. Geol.* **2020**, *429*, 106314. [[CrossRef](#)]
33. Huynh, D.H.; Bui, N.T.K.; Cao, H.B.; Pham, V.Q. Monitoring Riverbank Erosion in Can Gio Mangroves. In *Studies in Can Gio Mangrove Biosphere Reserve, Ho Chi Minh City, Viet Nam*; Mangrove Ecosystems Technical Reports No. 6; International Society for Mangrove Ecosystems (ISME): Okinawa, Japan, 2014; pp. 37–41.
34. Vien, N.N.; Le, Q.T. Erosion and Accretion in Can Gio Mangroves (1953 to 2010). In *Studies in Can Gio Mangrove Biosphere Reserve, Ho Chi Minh City, Viet Nam*; Mangrove Ecosystems Technical Reports No. 6; International Society for Mangrove Ecosystems (ISME): Okinawa, Japan, 2014; pp. 31–35.
35. Song-Hong-Co Ltd. *Technical Report of Geological Investigation for the Can Gio Coastal Urban Development Project*; Song-Hong-Co. Ltd.: Vung Tau, Vietnam, 2018. (In Vietnamese)
36. Schwarzer, K.; Diesing, M.; Larson, M.; Niedermeyer, R.O.; Schumacher, W.; Furmanczyk, K. Coastline Evolution at Different Time Scales—Examples from the Pomeranian Bight, Southern Baltic Sea. *Mar. Geol.* **2003**, *194*, 79–101. [[CrossRef](#)]
37. Kemp, A.C.; Horton, B.P.; Donnelly, J.P.; Mann, M.E.; Vermeer, M.; Rahmstorf, S. Climate Related Sea-Level Variations over the Past Two Millennia. *Proc. Natl. Acad. Sci. USA* **2011**, *108*, 11017–11022. [[CrossRef](#)] [[PubMed](#)]
38. Nguyen, V.L.; Ta, T.K.O.; Tateishi, M. Late Holocene Depositional Environments and Coastal Evolution of the Mekong River Delta, Southern Vietnam. *J. Asian Earth Sci.* **2000**, *18*, 427–439. [[CrossRef](#)]
39. Ta, T.K.O.; Nguyen, V.L.; Tateishi, M.; Kobayashi, I.; Saito, Y.; Nakamura, T. Sediment Facies and Late Holocene Progradation of the Mekong River Delta in Bentre Province, Southern Vietnam: An Example of Evolution from a Tide-Dominated to a Tide- and Wave-Dominated Delta. *Sediment. Geol.* **2002**, *152*, 313–325. [[CrossRef](#)]
40. Ta, T.K.O.; Nguyen, V.L.; Tateishi, M.; Kobayashi, I.; Tanabe, S.; Saito, Y. Holocene Delta Evolution and Sediment Discharge of the Mekong River, Southern Vietnam. *Quat. Sci. Rev.* **2002**, *21*, 1807–1819. [[CrossRef](#)]

41. Tanabe, S.; Thi Kim Oanh, T.; Nguyen, V.; Tateishi, M.; Kobayashi, I.; Saito, Y. Delta Evolution Model Inferred from the Mekong Delta, Southern Vietnam. In *SEPM Special Publication*; SEPM: Tulsa, OK, USA, 2003; Volume 76, pp. 175–188. ISBN 1-56576-086-7.
42. Nguyen, V.L.; Ta, T.K.O.; Tateishi, M.; Kobayashi, I.; Saito, Y. Holocene Evolution of the Mekong River Delta, Vietnam. *J. Geol. Soc. Jpn.* **2005**, *111*, XXI. [[CrossRef](#)]
43. Saito, Y. Deltas in Southeast and East Asia: Their Evolution and Current Problems. In *Global Change and Asia Pacific Coasts, Proceedings of APN/SURVAS/LOICZ Joint Conference on Coastal Impacts of Climate Change and Adaptation in the Asia-Pacific Region, APN, Kobe, Japan, 14–16 November 2000*; Mimura, N., Yokoki, H., Eds.; Ibaraki University: Ibaraki, Japan, 2001; pp. 185–191.
44. Galloway, W. *Process Framework for Describing the Morphologic and Stratigraphic Evolution of Deltaic Depositional System*; Special Publication No. 31; Society of Economic Paleontologists and Mineralogists (SEPM): Tulsa, OK, USA, 1975; pp. 127–156.
45. Van Loon, A.F.; Dijkma, R.; van Mensvoort, M.E.F. Hydrological Classification in Mangrove Areas: A Case Study in Can Gio, Vietnam. *Aquat. Bot.* **2007**, *87*, 80–82. [[CrossRef](#)]
46. Ha, Q.H.; Ma, C.C. *Geological Report for Ho Chi Minh City, Including Geological Map and Note of Mineral Resource, Scale 1/50.000*; Archives Department of Geology and Minerals of Vietnam: Hanoi, Vietnam, 1988. (In Vietnamese)
47. Hayashi, K.; Miyagi, T.; Kitaya, Y.; Vien, N.N. Geo-Ecological Rehabilitation Process of the Intensive Damaged Mangrove Forest in Can Gio District, Viet Nam. In *Annual Report of FY2005, the Core University Program between Japan Society for Promotion of Science and Vietnamese Academy of Science and Technology*; Ministry of Education, Culture, Sports, Science and Technology (MEXT): Tokyo, Japan, 2006; pp. 163–183.
48. Nguyen, C.T. Processes and Factors Controlling and Affecting the Retreat of Mangrove Shorelines in South Vietnam. Ph.D. Thesis, Kiel University, Kiel, Germany, 2012.
49. Nguyen, T.H. Burial Jars Tombs in the Southeast Vietnam—A New Discovery in Can Gio. Ph.D. Thesis, Institute of Social Science in Ho Chi Minh City, Ho Chi Minh City, Vietnam, 1997. (In Vietnamese)
50. EFEO. *Mission Archeologie du Delta du Mekong; Rapports de Mission*; EFEO: Paris, France, 2000.
51. EFEO. *Mission Archeologie du Delta du Mekong; Rapports de Mission*; EFEO: Paris, France, 2002.
52. Blott, S.J.; Pye, K. GRADISTAT: A Grain Size Distribution and Statistics Package for the Analysis of Unconsolidated Sediments. *Earth Surf. Process. Landf.* **2001**, *26*, 1237–1248. [[CrossRef](#)]
53. Folk, R.L. The Distinction between Grain Size and Mineral Composition in Sedimentary-Rock Nomenclature. *J. Geol.* **1954**, *62*, 344–359. [[CrossRef](#)]
54. Holtzapffel, T. *Les Minéraux Argileux: Préparation, Analyse Diffractométrique et Détermination*; Société Géologique du Nord: Lille, France, 1985.
55. Debenay, J.-P. Can the Confinement Index (Calculated on the Basis of Foraminiferal Populations) Be Used in the Study of Coastal Evolution during the Quaternary? *Quat. Int.* **1995**, *29–30*, 89–93. [[CrossRef](#)]
56. Bui, T.L.; Debenay, J.-P. Foraminifera, Environmental Bioindicators in the Highly Impacted Environments of the Mekong Delta. *Hydrobiologia* **2005**, *548*, 75–83. [[CrossRef](#)]
57. Stuiver, M.; Polach, H. Discussion-Reporting of <sup>14</sup>C Data. *Radiocarbon* **1977**, *19*, 355–363. [[CrossRef](#)]
58. Ramsey, C. Bayesian Analysis of Radiocarbon Dates. *Radiocarbon* **2009**, *51*, 337–360. [[CrossRef](#)]
59. Reimer, P.; Bard, E.; Bayliss, A.; Beck, J.; Blackwell, P.; Ramsey, C.; Buck, C.; Cheng, H.; Edwards, R.; Friedrich, M.; et al. IntCal13 and MARINE13 Radiocarbon Age Calibration Curves 0–50,000 Years Cal BP. *Radiocarbon* **2013**, *55*, 1869–1887. [[CrossRef](#)]
60. Lynch, J.; Hensel, P.; Cahoon, D. *The Surface Elevation Table and Marker Horizon Technique: A Protocol for Monitoring Wetland Elevation Dynamics, Natural Resource Report NPS/NCBN/NRR-2015/1078*; National Park Service: Fort Collins, CO, USA, 2015.
61. Le, X.T. La Zone Sud Du Delta Du Mékong: Sédimentation Actuelle et Évolution Récente. Ph.D. Thesis, University Bordeaux, Bordeaux, France, 1996.
62. Weaver, C.E. *Clays, Muds, and Shales*; Elsevier Science Publishers: Amsterdam, The Netherlands, 1989.
63. Le, X.T. Some Features of Distribution of Clay Minerals in the Mekong River Plain. *J. Geol.* **2006**, *295*, 51–66. (In Vietnamese)
64. Phan, M.H.; Ye, Q.; Reniers, A.J.H.M.; Stive, M.J.F. Tidal Wave Propagation along The Mekong Deltaic Coast. *Estuar. Coast. Shelf Sci.* **2019**, *220*, 73–98. [[CrossRef](#)]
65. Gagliano, S.M.; McIntire, W.G. *Reports on the Mekong River Delta*; DTIC: Lincoln, NE, USA, 1968.
66. Tjallingii, R.; Statterger, K.; Stocchi, P.; Saito, Y.; Wetzel, A. Rapid Flooding of the Southern Vietnam Shelf during the Early to Mid-Holocene. *J. Quat. Sci.* **2014**, *29*, 581–588. [[CrossRef](#)]
67. Wang, Y.; Cheng, H.; Edwards, R.L.; He, Y.; Kong, X.; An, Z.; Wu, J.; Kelly, M.J.; Dykoski, C.A.; Li, X. The Holocene Asian Monsoon: Links to Solar Changes and North Atlantic Climate. *Science* **2005**, *308*, 854–857. [[CrossRef](#)]
68. Renaud, J. *Etude d'un Projet Canal Entre le Vaico le Cuatieu, Excursion Reconnaiss, No. 3*; Saigon, Imprimerie du Government; Staatsbibliothek zu Berlin-Preußischer Kulturbesitz: Berlin, Germany, 1880; pp. 315–330. Available online: <https://www.deutsche-digitale-bibliothek.de/item/56SKQ4UNLQA64Z2IVWCTJJKWEIM4CDDY> (accessed on 10 August 2021).
69. NEDECO. *Technical Report of the Netherlands Delta Development Team Plan*; Netherlands Engineering Consultants (NEDECO): Amsterdam, The Netherlands, 1974.
70. Le, X.T.; Nguyen, M.P.L.; Nguyen, B.T.; Dang, H.V. *Southern Vietnam Land: Natural Conditions, Ecological Environment*; Truong, T.K.C., Ed.; National Political Publishing House: Hanoi, Vietnam, 2017. (In Vietnamese)
71. Tamura, T.; Saito, Y.; Sieng, S.; Ben, B.; Kong, M.; Sim, I.; Choup, S.; Akiba, F. Initiation of the Mekong River Delta at 8 Ka: Evidence from the Sedimentary Succession in the Cambodian Lowland. *Quat. Sci. Rev.* **2009**, *28*, 327–344. [[CrossRef](#)]

72. Lam, T.M.D. *Dongnai in Protohistory: The Meeting Place of Many Streams of Cultures*; Science of Dalat University: Dalat, Vietnam, 2020; Volume 10, pp. 52–69. (In Vietnamese)
73. Bui, C.H.; Nguyen, K.T.K.; Dang, N.K. *Prehistoric Archeology in the Southern Vietnam*; Science Social Publishers' House: Hanoi, Vietnam, 2019. (In Vietnamese)
74. Alongi, D. *Blue Carbon Coastal Sequestration for Climate Change Mitigation*; Springer: Cham, Switzerland, 2017.
75. Cahoon, D.R.; McKee, K.L.; Morris, J.T. How Plants Influence Resilience of Salt Marsh and Mangrove Wetlands to Sea-Level Rise. *Estuaries Coasts* **2021**, *44*, 883–898. [[CrossRef](#)]
76. Woodroffe, C.D. *Coasts: Form, Process and Evolution*; Cambridge University Press: New York, NY, USA, 2003. ISBN 0521812542.
77. Tamura, T.; Saito, Y.; Nguyen, V.L.; Ta, T.K.O.; Bateman, M.D.; Matsumoto, D.; Yamashita, S. Origin and Evolution of Intertributary Delta Plains; Insights from Mekong River Delta. *Geology* **2012**, *40*, 303–306. [[CrossRef](#)]
78. Griffiths, M.; Johnson, K.; Pausata, F.S.R.; White, J.; Henderson, G.; Wood, C.; Yang, H.; Ersek, V.; Conrad, C.; Sekhon, N. End of Green Sahara Amplified Mid- to Late Holocene Megadroughts in Mainland Southeast Asia. *Nat. Commun.* **2020**, *11*, 4204. [[CrossRef](#)] [[PubMed](#)]
79. Tamura, T.; Horaguchi, K.; Saito, Y.; Nguyen, V.L.; Tateishi, M.; Ta, T.K.O.; Nanayama, F.; Watanabe, K. Monsoon-Influenced Variations in Morphology and Sediment of a Mesotidal Beach on the Mekong River Delta Coast. *Geomorphology* **2010**, *116*, 11–23. [[CrossRef](#)]
80. Truong, V.B.; Nguyen, K.D. Effects of River-Sea Dynamics Processes on the Accretion-Erosion and Shoreline Changes in Cua Lap and Loc An Estuary. *Vietnam. J. Hydro Meteorology* **2012**, *618*, 9–15. (In Vietnamese)
81. Nguyen, Q.D.A.; Dinh, V.D.; Tanaka, H.; Nguyen, T.V. Elongation of Sand Spit at the Loc An River Mouth, Southern Vietnam. *Doboku Gakkai Ronbunshuu B* **2018**, *74*, 695–700. [[CrossRef](#)]
82. Gugliotta, M.; Saito, Y.; Nguyen, V.L.; Ta, T.K.O.; Tamura, T. Sediment Distribution and Depositional Processes along the Fluvial to Marine Transition Zone of the Mekong River Delta, Vietnam. *Sedimentology* **2019**, *66*, 146–164. [[CrossRef](#)]